Development of a Long Endurance Mini-UAV : ETERNITY

Murat Bronz, Gautier Hattenberger, Jean-Marc Moschetta

Development of a Long Endurance Mini-UAV: ETERNITY

Murat Bronz[1*], Gautier Hattenberger[1a] and Jean-Marc Moschetta[2b]
[1]l'Ecole National de l'Aviation Civil, Toulouse, France
murat.bronz@enac.fr, gautier.hattenberger@enac.fr
[2]Institut Supérieur de l'Aéronautique et de l'Espace, Toulouse, France
jean-marc.moschetta@isae.fr

ABSTRACT

This study presents the effort given for the first prototype of a *Long Endurance Mini UAV* concept called *Eternity*. A multi-disciplinary conceptual aircraft design program called *CDSGN* is developed and used for the design of the *Eternity*. Unlike the traditional design methods that uses statistical data from the previous well-flown aircrafts, *CDSGN* analyses numerous aircraft candidates and simulates each candidate for the   given mission definition and outputs the corresponding performance. The unique property of the presented design methodology comes from a computationally fast and physically accurate modelling of the aerodynamic characteristics of each candidate by using a modified version of a vortex lattice program called AVL from Mark Drela. Two types of configurations have been analysed for the *Eternity* design, conventional and flying-wing. A wide envelope of variable design parameters used for both configurations such as wing surface area, cruise speed, battery capacity, different airfoils, etc... Integration of solar cells, and the management of solar energy is also considered for every candidate. Only the wing span size has been limited to one meter. Additionally, the on-board avionics and payload weights and sizes are fixed for every candidate as they are independent of the design. Analyses by *CDSGN* concluded the dominance of the conventional configuration for the given long endurance mission performance both on solar and non-solar conditions. Optimum wing surface area and the on-board battery energy found interactively by a post-filtering program developed in-house. A custom airfoil family, transitioning along the span, have been designed specifically for the corresponding local Reynolds number for specific spanwise locations. A wind-tunnel campaign is performed with a full-scale model and first flight tests have been performed in order to show the feasibility of long endurance flights.

1. INTRODUCTION

Endurance performance enhancement of mini and micro UAVs has been a common interest which relies on many aspects of the design. Traditional conceptual design methods such as Raymer[9] and Roskam[10] generally leads the UAV design to a safe and robust selection which is not always sufficient to push the performance to its limits. The challenge of designing a mini-UAV for long-endurance mission requires to think out of the box for the for the design method.

The multidisciplinary nature of UAVs demand for a better understanding of the interactions between each discipline. Modeling of these interactions physically accurate and yet computationally fast becomes the main challenge for a new design method.

This study will present the design optimization of a one-meter UAV, called *Eternity*, which shows the feasibility of an electric powered Long-Endurance MAV concept. The particular interest is on the developed CDSGN conceptual aircraft design tool specialized on MAV scale. Each of the subsystems (e.g. aerodynamics, structure, propulsion, control,...) modelled seperately in order to see their final effect on the performance of the vehicle.

---

*Assistant Professor in Applied Aerodynamics
[a]Assistant Professor in Flight Dynamics
[b]Professor in Aerodynamics

2. CDSGN : THE CONCEPTUAL DESIGN TOOL

CDSGN [4] is a multi-disciplinary conceptual aircraft design program. The core aerodynamic calculations are done by using a modified version of AVL program [7], which uses vortex lattice method. Modifications include the airfoil viscous drag addition coming from an XFOIL[6] database, fuselage skin friction drag with flat plate approximation [8], and stall information according to the maximum local lift coefficients of the particular airfoils at corresponding Reynolds number.

It uses a computationally fast, yet physically realistic method whose results have been verified with several wind-tunnel and flight tests[4, 3]. Figure 1 shows the brief flow chart of the program.
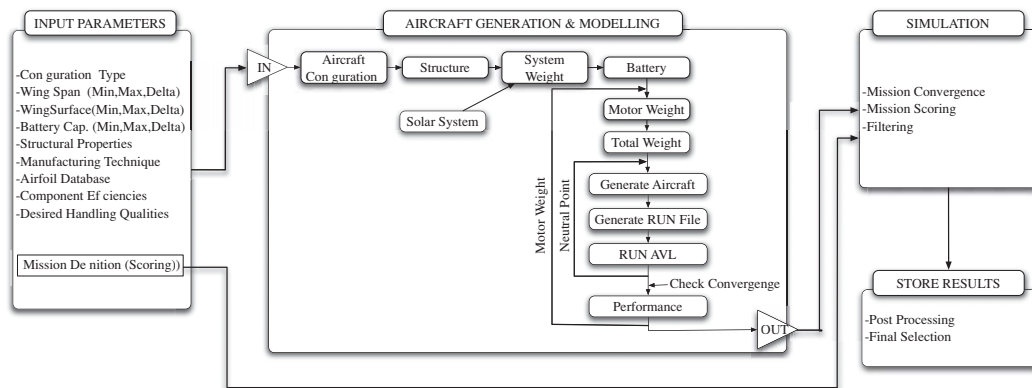

Figure 1: Brief flowchart of *CDSGN* program.

3. DESIGN ENVELOPE

In order to see the endurance and range performance limits of a one-meter aircraft, various configuration "*cases*" are investigated by CDSGN. Table 1 shows the main variables and their ranges used as an input on the program. Each of these variables is examined on different aircraft configurations with different airfoils, wing planforms, energy systems and stability characteristics. This facilitates the performance comparison of each *case* for the whole variable space. Comparisons will be explained in the related sections.

Table 1: The range of main variables used for the design envelope of *Eternity*.

Main Variables	Range	
Aircraft Configuration	Conventional or Flying-Wing	
Energy Source	Battery only or + Solar energy	
Wing Surface Area	$0.05 - 0.2$	m^2
Flight Speed	$8 - 20$	m/s
Battery Energy	$20 - 210$	Wh

3.1 Configuration Selection

Although several aircraft configurations exist, in order to keep the design simple and parametric over the main variables shown in table 1, only conventional and flying wing configurations are considered. Each aircraft is generated automatically by *CDSGN* for each single main variable value. Figure 2 shows some of the automatically generated aircraft configurations as an example.

The main objective of this design phase is to see the high-end performance capabilities of each configuration.
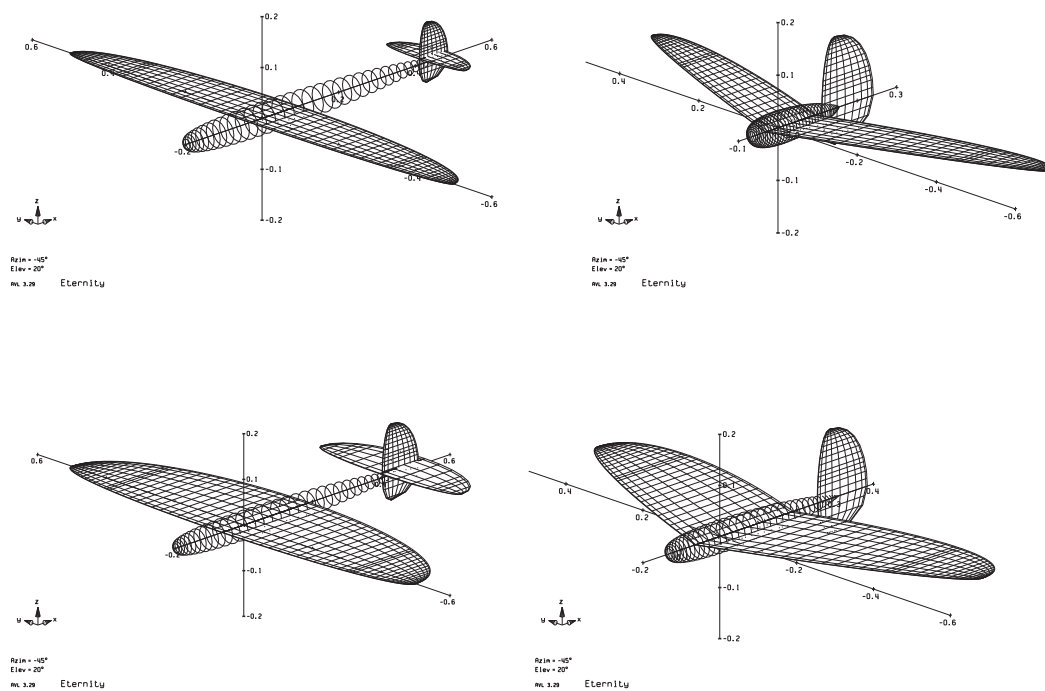
Figure 2: Examples of some automatic generated aircraft configurations by *CDSGN*.

Figure 3 shows the theoretical performance potentials of 1-meter conventional aircraft (on the left) within the initial specified design constants.The on-board energy, relatively represented by the circle radius, varies between 20 *Wh*-210 *Wh* corresponding to 0.1 *kg-1.5 kg* pure battery mass respectively. It can be seen that as the wing area increases, the saturation of maximum on– board energy reduces the maximum endurance and range performance. This was an expected behaviour; the performance of greater surface area configurations can easily be increased by increasing the maximum on-board energy limitation. However, the ease of operation (like hand launching) and certain UAV regulations favour keeping the total mass of the UAV under 2 *kg* [2].
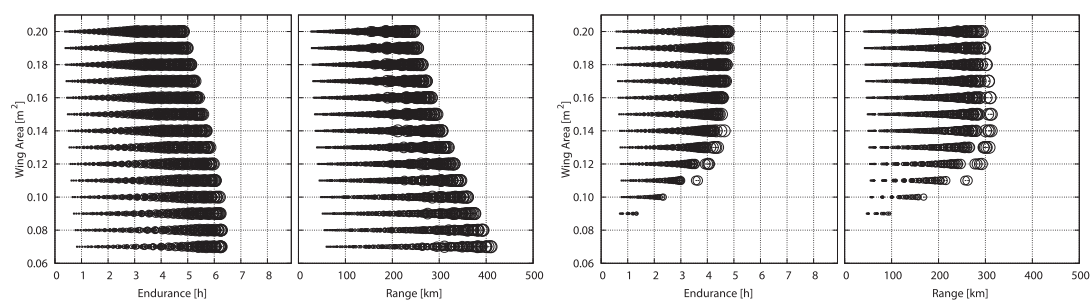

Figure 3: Performance plot of 1-meter conventional aircraft on the left and 1-meter flying wing aircraft on the right in various specifications with only battery. Circle radius represents the relative on-board energy being between 20 *Wh* and 210 *Wh* for min and max size.

On the right of Figure 3, the same type of performance plot for flying wing configuration is presented. In contrast to the conventional configuration, flying wing configuration tends to have better endurance and range performance for increased wing area. This is mainly due to having a lower maximum lift coefficient CL_{max} in trimmed level flight conditions, in comparison to conventional configuration because of airfoil type and not having a separate horizontal tail.

3.1.1 Effect of Solar Energy

In order to see the effect of using Solar Energy, the same type of analysis was done while taking into account the additional weight and limitations of solar cells, such as the maximum power point tracker board, connection cables, etc.
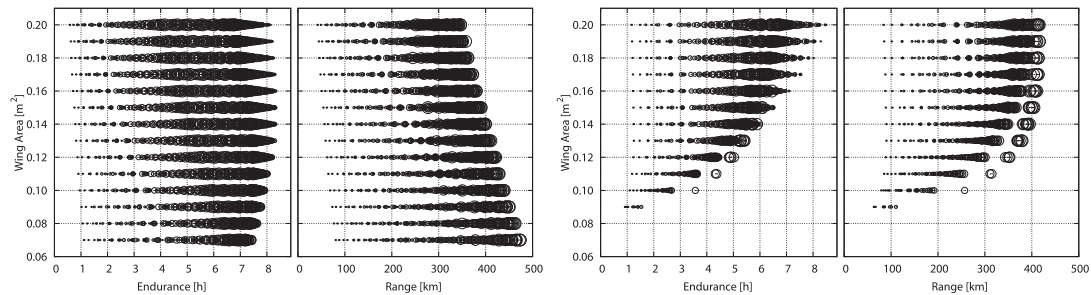

Figure 4: Performance plot of 1-meter conventional aircraft on the left and 1-meter flying wing aircraft on the right in various specifications with battery and solar cells. Circle radius represents the relative on-board energy being between 20 *Wh* and 210 *Wh* for min and max size.

Figure 4 shows the endurance and range performance of 1-meter conventional (on the left) and flying-wing (on the right) configuration with on-board battery and solar cells. For the conventional configuration, the increase of both endurance and range performance is clearly visible if it is compared with figure 3. Solar energy enhances the endurance up to 8 + *hours*, where it was around 6 *hours* before. The range increases 100-150 *km* on average. Additionally, maximum endurance is evenly distributed over the various wing areas. The need for additional on-board energy is still visible for the bigger wing areas, but this time with the effect of solar cells covering the wing area, it is possible to use a smaller amount of on-board energy in order to be light. This ensures reduction of required flight power, which is maintained by the solar cells on the big wing surface. This is the reason why we see the configurations with smaller on-board energy having better endurance performance for the bigger wing surfaces, although the bigger wing creates more drag than the smaller wings at the same flight speed.

For the flying-wing configuration, the endurance performance seems to increase from 4.5 *hours* to 8 *hours* in certain *cases*. The *cases* with bigger wing areas, which carry small amounts of on-board energy, have slower cruise speeds and obtain more advantages from the solar energy. It should still be noted that these *cases* are too sensitive for flight conditions and environment such as a small amount of difference in the cruise flight speed or a decrease in solar irradiation, which end up shifting the performance values dramatically.

3.1.2 Conventional or Flying-Wing ?

Previous figures showed that both conventional and flying wing configurations are able to achieve 8 + *hours* of flight time with the help of solar energy. However, flying wing configuration is only able to reach that goal for a limited number of *cases*, while conventional configuration has well proven that the goal is reachable for a wide range of design variables. This is mainly due to the airfoil performance and the longitudinal trim issues that are limited with the flying wing configuration, especially at higher lift coefficients. This proves that the conventional configuration will be more robust for a real-world application, where the conditions and environment change constantly. Additionally, non-solar performance of conventional configurations highly outperformed flying wing configurations on average. While making these conclusions, the whole envelope of design variables has taken into account for both configurations. It should be also noted that the best performing candidates have to be also suitable for the whole mission requirements, such as maximum wind speeds to cope with, minimum landing speed, hand launch possibility, etc... Finally, the conventional configuration is selected as it outperformed the flying-wing configuration in these mission requirements.

3.2 Required Optimum Energy (On-Board)

The weight of the stored on-board energy is one of the key points in enhancing the platform performances, so it is important to select the optimum on-board energy that will give the best range and endurance performances for both solar and non-solar conditions. Table 2 shows the general specifications of off-the-shelf batteries. Lithium-Polymer batteries are used in all of the analyses, since Lithium-Sulfur batteries are almost impossible to obtain for our project because of their supplier policies(Sion Power [1]). As a result of several discharge tests, the specific energy is taken as 190 *Wh/kg* different from the general table.

In order to see the effect of on-board energy on performance, the same analyses done previously are plotted in a different way. Figure 5 shows the endurance and range performance of different designs for non-solar configuration (on the left) and solar configuration (on the right) versus on-board energy. For non solar configuration, the effect of additional on-board energy is getting to a saturation around 150 *W h* , and above that value carrying more energy on board has no advantage for endurance performance. For the range performance, although there is a reduction on the increase, it keeps increasing with the additional energy. Caution should be given to the point that the given battery volume after a certain value will be impossible to carry on-board due to the size of the plane.

Table 2: Typical battery specifications.

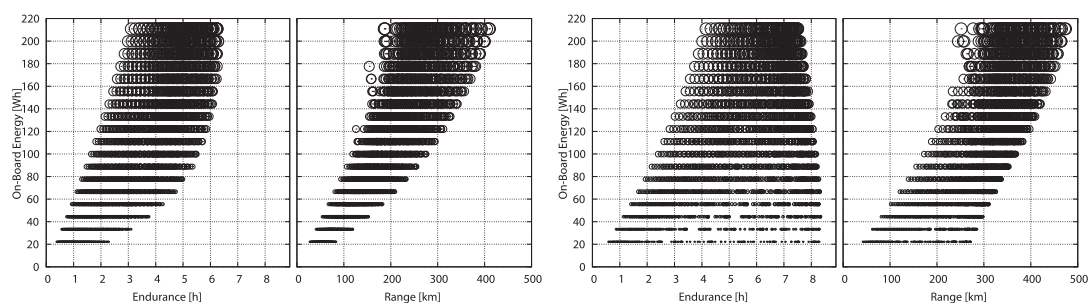|		Ni-C d	Ni-Mh	Li-P o	Li-S
Specific E nergy	(W h/k g)	40	80	180	350
Energy Densit y	(W h/l)	100	300	300	350
Specific P ower	(W/ kg)	300	900	2800	600

Figure 5: Effect of on-board energy on endurance and range performance, on the left with battery-only and on the right with solar energy addition.

On the right of figure 5, for solar configurations, it is assumed that 70% of the wing area is covered with solar cells. As seen, solar energy has a big influence on endurance performance, especially for the configurations that have low on-board energy, thus lower weight. This result was already presented in the previous analysis, but the clear relation with the on-board energy has just been shown again. For solar configurations, an optimum on-board energy of 50 *Wh* gives the best endurance performance. In these calculations, the specific energy of the battery was chosen as 190 *Wh/kg*, which results in around 250 *gr* of battery weight for maximum endurance performance of a 1 *m* spanned aircraft in solar conditions. For the range performance, the behaviour is not different from the non-solar flight results. The more on-board energy that is carried on the aircraft, the better the range performance.

4. DESIGN PHILOSOPHY

It was shown in the previous section that one configuration will not be capable of having the optimum performance in both endurance and range performance at solar and non-solar conditions. Designing the aircraft for only one particular condition will make it fail during almost all flight conditions different from the design point. The main focus of the design is to have a long-endurance aircraft, and

the design philosophy is to obtain long-endurance performance in the operational cases as well, and not only on one particular condition.

4.1 Idea of Variable Configuration

It is possible to design different aircraft for different missions and conditions, however *Eternity* long endurance mini UAV should be as compact as possible. Therefore, concentrating on one wing planform which can be used with two different fuselages and various battery packages was found to be the most promising option. Finally, there will be different systems that will be appropriate for various missions and flight conditions.

The battery pack is designed as a wing joiner simultaneously. The sizing of the joiner battery pack is also a key point, as it plays a big role on the wing planform and airfoil limitations. AMI cell[1] ($155mm \times 60mm \times 4mm$), 4.5 *Ah* 3.7 *V* seemed to be the best fit for the wing joiner battery pack. Finally, a four cell battery pack is built in the joiner.

5. DESIGN DETAILS

With the battery cell type selected, the on-board energy was partially decided as a result. The wing joiner will consist of a four cell 4.5 *Ah* (66 *W h*) battery, which is suitable for long endurance mission in a sunny day. For overcast weather or a long range mission, it is preferable to use 2 packs (132 *W h*) of batteries. In order to fit an additional battery pack into the system, the fuselage has to be enlarged. This is not going to be beneficial for the long endurance version, as it will cause some additional drag. These points indicate that two separate fuselages are needed in order to optimize the system for both endurance and range missions using the same wing and tail parts. This decision also makes it possible to use different propulsion systems (propeller, motor, speed controller) optimized particularly for each mission, rather than compromising between them.
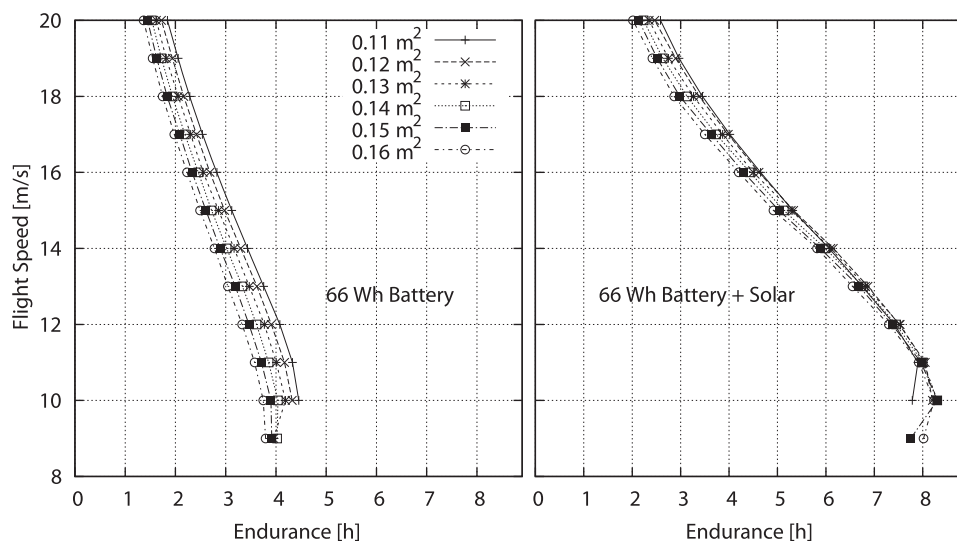

Figure 6: The effect of various flight speed and wing area on the endurance performance of non-solar and solar configurations with 66Wh of on-board energy.

Figures 6 and 7 shows the endurance performance for various wing areas and flight speeds for 66 *W h* and 132 *W h* on-board energy in both solar and non-solar conditions. The same performance evoluation is done for the range and taking into account the four conditions and additional operational requirements (such as take-off and landing), 0.14 *m*2 of wing area performs the best.
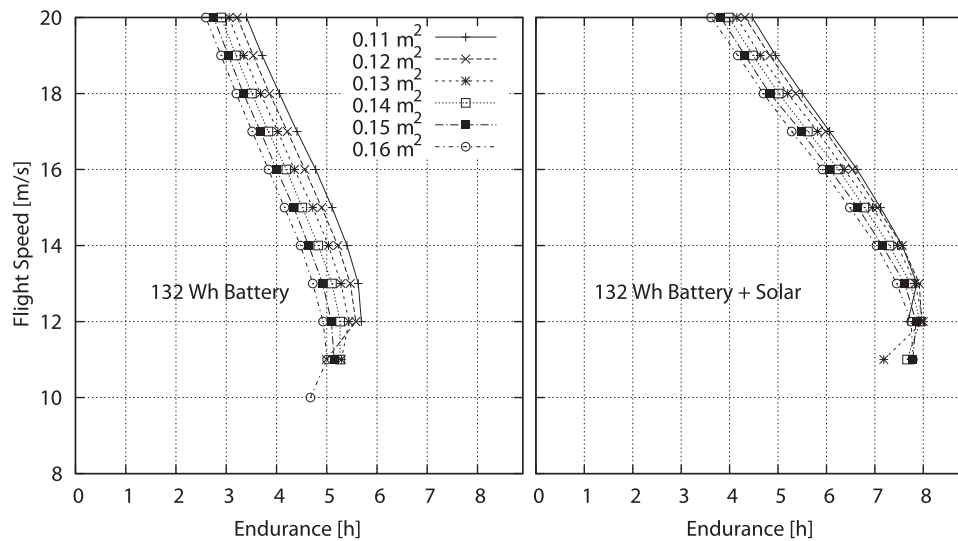
---

[1] http://www.amicell.co.il/

Figure 7: The effect of various flight speed and wing area on the endurance performance of non-solar and solar configurations with 132Wh of on-board energy.

5.1 Design of the Airfoil Family

In the conceptual design phase, suitable airfoils were selected as candidates by examining their maximum power coefficient ($C_l^{1.5}/C_d$) values. Then, the effect of different airfoils on endurance and range performance are investigated. Finally, by using the best existing airfoil as a starting geometry, a custom airfoil is designed by using XFOIL[2] according to the main requirements of the design. PKMB500 airfoil is designed by Philip Kolb, which outperformed all previous airfoils existing in the selected database for our application.

The main reason why PKMB500 can give better results than its precedents relies on the fact that it is designed according to the *Eternity*'s specifications. The wing area was designated 0.145 m^2, and the battery weights were determined by the selected optimum capacities for solar and non-solar conditions. Since almost all of the main parameters of the design have been selected, it is easy to calculate the $Re\sqrt{C_L}$ of the mean aerodynamic chord via equation 1 and later define all of the particular chord lengths proportionally.

$$Re\sqrt{C_L} = \frac{1}{\mu}\sqrt{\frac{2\rho W}{AR}} \tag{1}$$

For the two configurations of *Eternity* (66 $W\,h$ and 132 $W\,h$), calculated mean $Re\sqrt{C_L}$ are 90k and 110k respectively. After obtaining the working regime, priority is given to the$((C_l^{1.5}/C_d)_{max})$ value of the airfoil, as the endurance performance is the main objective for the design. SD7037 airfoil is selected as a reference because it is widely known and used in soaring competition gliders. By using the QDES routine of XFOIL, the laminar run on the top surface is extended by increasing the aft-loading the airfoil. The transition ramp slope is slightly reduced and the pressure distribution at the bottom end is increased. This resulted an increase on the pitching moment increase on the final airfoil ($\Delta C_m = 0.025$), which was acceptable as the conventional configuration was selected. The suction peak is smoothed, resulting in a better continuity of the flow and postponement of the transition. It is known that the bubble loss contributes significantly to the form drag on the low-Reynolds airfoils. One way of reducing the bubble size is to move it farther upstream by forcing the transition earlier. However, it will not be beneficial to completely prevent the occurrence of the bubble, because the laminar flow will be shortened dramatically. There is an optimum position for the bubble placement and size that corresponds to the minimum drag, and in low Reynolds airfoil design the control of the bubble becomes more critical compared to minimizing skin friction [5]. Figure 8 shows the pressure distributions of the SD7037 and the new designed PKMB500 airfoil at different lift coefficients.
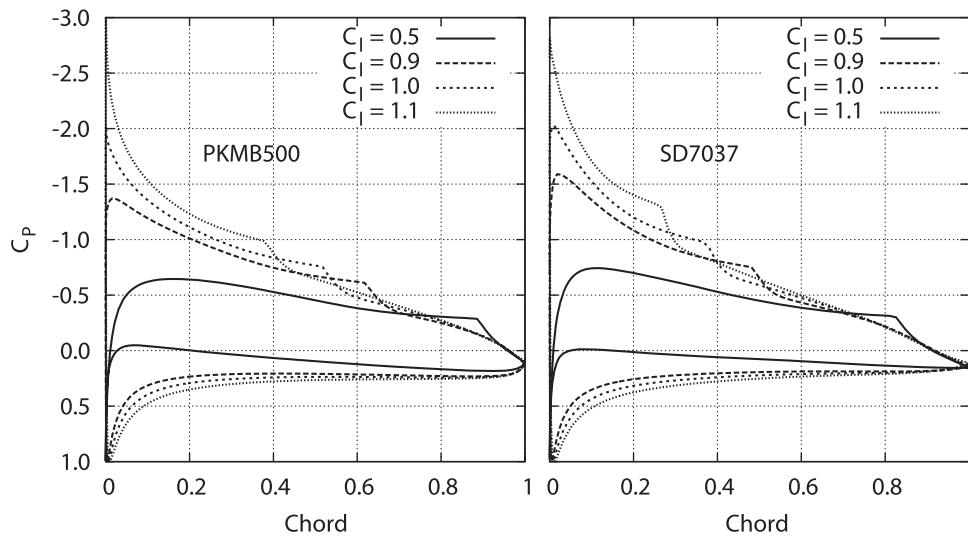
---

[2]xfoil.mit.edu

Figure 8: Pressure distribution change for PKMB500 and SD7037 airfoils at Re = 150k.

In order to improve the airfoil performance along the span and decrease the viscous drag caused by inappropriate airfoil location, a series of airfoils are designed by referencing PKMB500.

PKMB803 is designed particularly for its own working regime, which is $Re\sqrt{C_L}$ = 30000. Figure 9 shows the placement of the designed airfoils along the span, with a drag comparison of each with the root airfoil PKMB500 in their corresponding flow regime. Having a smooth surface on the wing while transitioning from PKMB500 to PKMB803 on an elliptical planform created a dominant restriction on the thicknesses of PKMB601 and PKMB702. As the chord distribution has already been fixed, adding the root and the tip airfoil thickness values automatically defines the thickness distribution. With this thickness restriction, the only way found to slightly improve the performance of the middle airfoils was to compromise from the maximum lift coefficient and concentrate on the cruise coefficient regime corresponding to best endurance, which is around C_L = 0.9- 1.0.
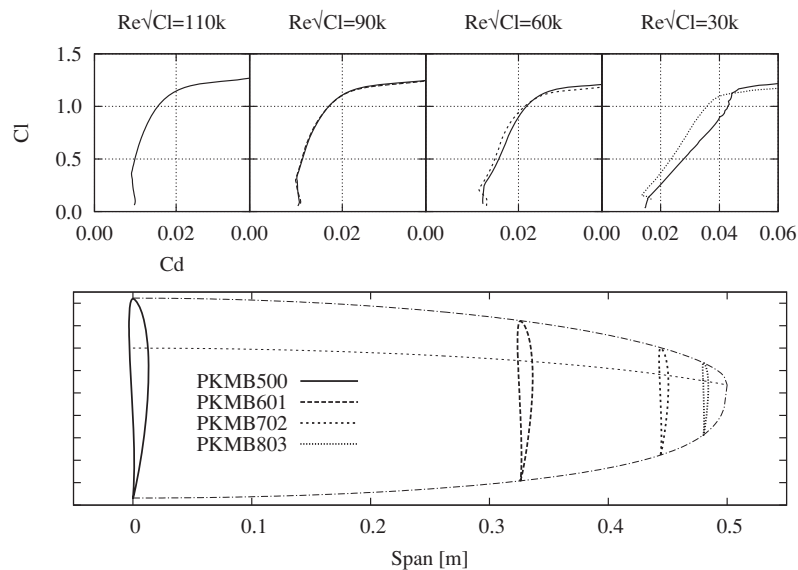

Figure 9: Placement of each airfoil is shown along the half span. The upper graphs shows the C_l vs C_d plots of each airfoils at their corresponding working regimes with the comparison to the root PKMB500 airfoil. The planform shown is given as demonstration and the real planform is shown later in figure 10.

Final dimensions of the two *Eternity* versions are shown in the figure 10, with their specifications in table 11.
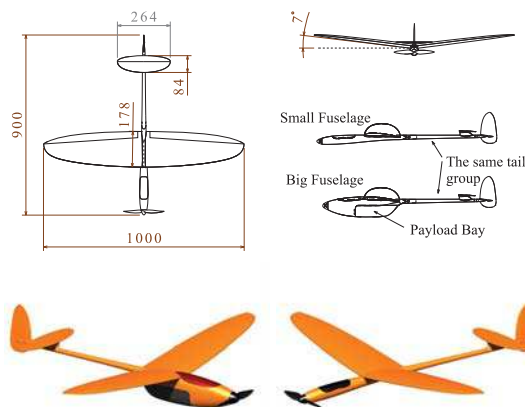

Figure 10: *Eternity* design with two different fuselages.

		Small	Big
Wing Area	[m^2]	0.145	0.145
Total Mass	[kg]	0.85	1.35
Length	[m]	0.9	0.87
Wing AR	[−]	6.89	6.89
Horizontal tail AR	[−]	4.0	4.0
Vertical tail AR	[−]	2.0	2.0
Horizontal tail volume	[−]	0.4	0.4
Horizontal tail arm	[m]	0.45	0.45
Vertical tail volume	[−]	0.03	0.03
Vertical tail arm	[m]	0.53	0.53

Figure 11: Geometrical specifications of the two *Eternity* configurations.

6. WIND TUNNEL TESTS

In order to obtain the aerodynamic characteristics of the aircraft in a controlled environment, a wind-tunnel campaign was conducted at ISAE S4 wind-tunnel. An internal six component force and moment balance was used for the measurements.

Instead of manufacturing a separate wind-tunnel model, a fully equipped ready-to-fly version was manufactured and used for the tests. This was initiated in order to save some time, as one particular model takes one person about 3-4 weeks to build, including all the necessary equipment integration. Figure 12 shows the mounting of the aircraft in the wind-tunnel. The control surfaces and the motor of the aircraft were controlled by the onboard Paparazzi autopilot, which was connected to a computer via serial connection.

The experiments are conducted for different speeds in order to see the performance of the aircraft at each flight speed and evaluate the aerodynamic characteristics for a wider flight range. For each wind-tunnel speed the aircraft pitched from -6 to 12 degrees in order to obtain the performance polars.
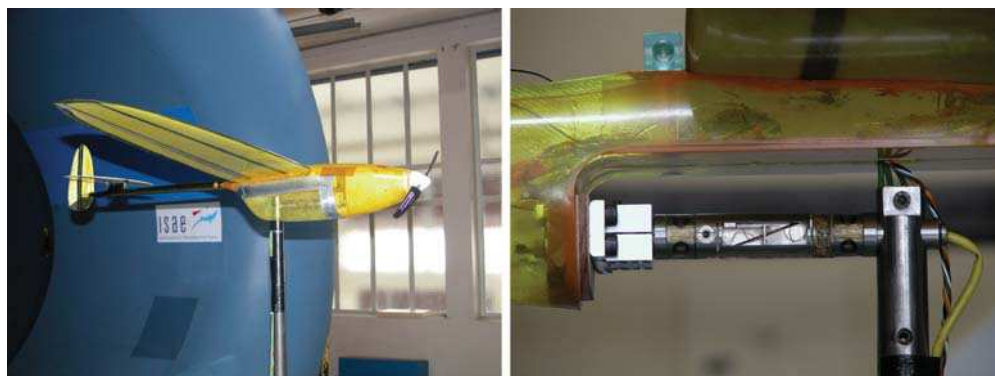

Figure 12: The mounting of Eternity on S4 Wind-tunnel, the payload compartment of the Eternity has been used for the mounting of the internal balance, and then the payload bay covered in order to protect the balance and to have the accurate fuselage shape.

The expected influence of the Reynolds number is clearly visible in figure 13; as the flight speed decreases, both the range (C_L/C_D) and the endurance ($C_L^{1.5}/C_D$) performance decrease. Attention

should be given to the fact that figure 13 does not present the equilibrium condition performance. In order to have the equilibrium plot, elevator deflection has to be taken into account as well as at which it corresponds to zero pitching moment.

According to the previous analyses, the best endurance performance is achieved at $C_L = 0.9 - 1.0$, where the cruise speed corresponds to $12.5 - 13.0$ m/s, which is really close to stall speed of the big configuration that is 11.5 m/s. In real-life applications, for mini-micro UAV scales that are generally flying around $10 - 25$ m/s, sustaining airspeed accurately is really hard when the small momentum of the aircraft and the big ratio of the wind gusts to the flight speed are considered. Therefore, increasing the flight speed results in a reasonable safety margin. In the end of this decision, the cruise speed is selected as 14 m/s.
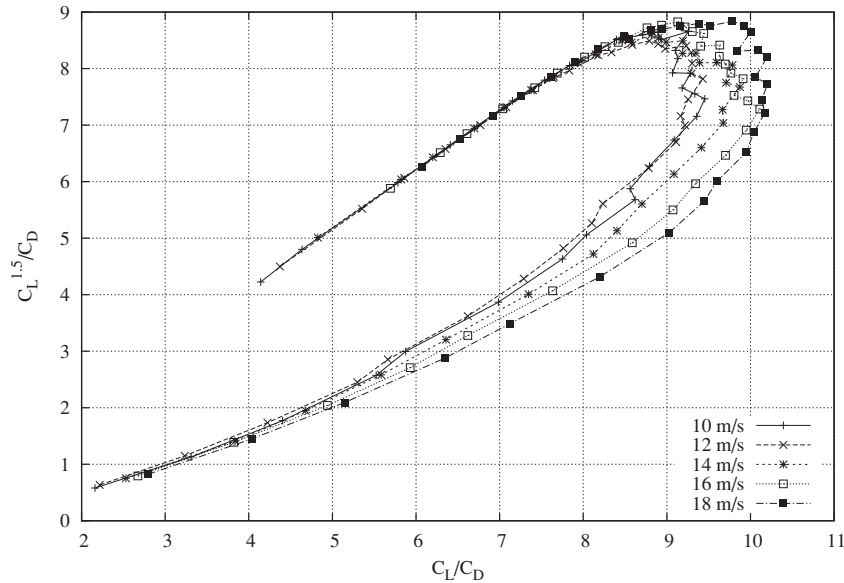

Figure 13: Effect of flight speed on the range and endurance performance characteristics.

6.1 High Speed Performance

In order to have a safety margin for the stall, the cruise speed is increased to 14 m/s, where the lift coefficient corresponds to $C_L = 0.76$ for the aircraft(big configuration). However, in the conceptual design of the *Eternity*, the cruise speed was chosen to be where the endurance is at its maximum value. The corresponding cruise lift coefficient is around $C_L = 0.9 - 1.0$. This region was always the most important region while selecting and designing the airfoil sections.

However, in real-life applications there will be situations where the aircraft will have to go out of this design region, such as penetration into wind or reaching a point faster for priority. In order to improve the high speed performance of the aircraft, the low lift coefficient region of the airfoil sections has to be improved. The most important thing in doing this is to avoid reducing the performance at and around the higher lift coefficients that correspond to cruise. The main performance reduction for the PKMB500 airfoil at high speed (over 18 m/s in our case) comes from the extended laminar bubble located at the aft part of the airfoil's top surface. This was already foreseen in the design phase of the airfoil in XFOIL program.

In order to prevent this, a turbulator strip will be used around 75% of the chord all along the wing span, which will turn the flow from laminar to turbulent before the laminar bubble occurs. In order to see the effect of different thickness and locations of the turbulator strips, five experiments were conducted, as shown in figure 14, with a strip tape 1.57 mm wide and 0.15 mm thick. In order to increase the thickness, two and three layers were taped on top of each other. As seen in figure 14, the high lift coefficient regime, where the cruise flight will be, is not affected by the turbulator strip, and at the point where the 18m/s flight will be $(C_L = 0.46)$ there is a drag reduction of $\Delta C_D = 0.0085$, which corresponds to 18.2% of improvement for the range performance at 18m/ s. The development of the laminar bubble starts before the strip, so that the strip does not harm the cruise

lift coefficients but still reduces the drag over the lower lift coefficients where the higher speed flight will be. Additionally, figure 15 shows the endurance $(C_L^{1.5}/C_D)$ performance versus the (C_L/C_D) range performance for various turbulator strip thicknesses and locations. The best performing combination is one layer strip (t = 1) at 75% location. The points shown with the arrows correspond to the equilibrium point where $C_L = 0.46$, as it can be seen the range performance is improved about 20% without affecting the endurance performance at all. This concludes that having a turbulator strip at every flight is beneficial.
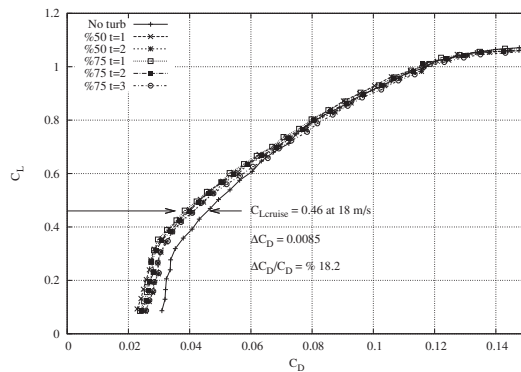

Figure 14: Turbulator effect at 18m/s for different thicknesses t = 1,2,3 and chord locations %50 and %75 all along the span.
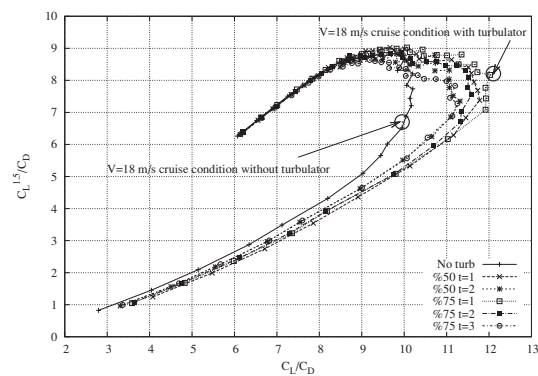
Figure 15: Turbulator effect at 18m/s.

7. FLIGHT TESTS

Close to 10 *hours* of flights have been recorded. The first prototype that has also been used in the wind-tunnel tests is used for the flights. Only one battery has been used, nevertheless the total weight of the aircraft (in flight ready state) was *930g,* just a bit heavier than the expected single battery configuration by 100 *g*. Additionally, the big fuselage is used as the thin fuselage was not build at that time. The longest flight that has been achieved was 2 *hours* and *7minutes* by using 54 *Wh* of energy. The battery has given only 81% of its expected energy. The maximum glide ratio *(L/D)* and the power coefficient $(C_L^{1.5}/C_D)$ is found to be 13.9 and 13.0 from the glide tests.

Considering all the differences of the test configuration compared to the design configurations, the flight test results act as a reference point rather than a direct comparison.

Table 3: Expected performance of the two Eternity configurations.

		Small	Big
Cruise Speed	[m/s]	11.5	14.0
Cruise Lift Coefficient	[−]	0.71	0.76
Stall Speed	[m/s]	9.2	11.6
Max Bank Angle at V_{cruise}	[deg]	50.0	46.0
Turn Radius at Max Bank	[m]	11.3	19.3
Battery capacity	[Wh]	62.5	125
Payload Mass	[kg]	0.05	0.10
Total Masss	[kg]	0.85	1.35
Solar Conditions			
Endurance	[h]	7.48	6.2
Range	[km]	309	312
Non-Solar Conditions			
Endurance	[h]	3.3	3.92
Range	[km]	138	197

8. OVERALL DESIGN CONCLUSION

The main objective of this study was to show the feasibility of the *Long Endurance Mini UAV* concept. *Eternity* shows a great perspective about what can be achieved with a one-meter aircraft. Finally, it can be concluded that with a one-meter aircraft that fits into an even smaller half meter carry-on luggage, 4 hours of flight are possible, and this can be enhanced up to 8 hours on a sunny day with the help of solar cells.

ACKNOWLEDGEMENTS

REFERENCES

[1] Sion power, the rechargeable battery company.

[2] Arreté du 21 mars 2007 relatif aux aéronefs non habités qui evoluent en vue directe de leurs opérateurs, May 2010.

[3] Murat Bronz. Experimental comparison of 1-meter conventional, pusher and tractor flying wing aircraft configurations in s4 wind-tunnel. Technical report, ISAE, 2009.

[4] Murat Bronz. *A Contribution to the Design of Long-Endurance Mini Aerial Vehicles*. PhD thesis, l'Ecole National de l'Aviation Civile, 2012.

[5] Mark Drela. Low-reynolds number airfoil design for the mit daedalus prototype: A case study. *Journal of Aircraft*, 25(8):724–732, August 1988.

[6] Mark Drela. An analysis and design system for low reynolds number airfoils. In University of Notre Dame, editor, *Conference on Low Reynolds Number Airfoil Aerodynamics*, June 1989.

[7] Mark Drela and Harold Youngren. Athena vortex lattice, Sep 2004. [8] Dr.-Ing. S. F. HOERNER. *Fluid-Dynamic Drag*. 1965.

[9] Daniel P. Raymer. *Aircraft Design : A Conceptual Approach*. American Institute of Aeronautics and Astronautics,Inc., Virginia,VA, 2006.

[10] Jan Roskam. *Airplane Design*. DAR Corporation, Lawrence, Kansas, 2000.

---

[3]www.delair-tech.com
[4]www.toulouse-tech-transfer.com